A combined approach for modeling particle behavior in granular impact damper using discrete element method and cellular automata

doi: 10.1007/s10999-016-9344-3

A Combined Approach for Modeling Particle Behavior in Granular Impact Damper using Discrete Element Method and Cellular Automata

Toshihiko Komatsuzaki[1,*] and Yoshio Iwata [1]

[1] *Institute of Science and Engineering, Kanazawa University*
Kakuma-machi, Kanazawa, Ishikawa, 920-1192 Japan

* Corresponding author
Phone: +81-76-234-4673; Fax: +81-76-234-4676
toshi@se.kanazawa-u.ac.jp

Abstract

A particle impact damper is a vibration absorber type that consists of a container attached to a primary vibrating structure. It also contains many particles that are constrained to move inside the container, whereby the damping effect can be obtained by collision between particles and the container. The discrete element method (DEM) has been developed for modeling granular systems, where the kinematics of each particle are calculated numerically using the equations of motion. However, the computational time is significant since the algorithm checks for particle contacts for all possible particle combinations. The use of a cellular automata (CA) modeling technique may provide increased computational efficiency due to the local updating of variables, and the discrete treatment of time and space. In this study, we propose a new approach combining DEM with CA for modeling a granular damper under a forced excitation. We use DEM to describe the particle motion according to the equations of motion, while CA is introduced for the particle contact checks in discrete space. We also investigate the effect of simplification in the contact force model, which allows the unit time step of numerical integration to become larger than that used in the strict model. It is shown that the suggested particle contact scanning method and the force approximation model contribute to the reduction of the computational time, and neither degenerates the calculation accuracy nor causes the numerical instability.

Key words

Particle Impact Damper, Granular materials, Discrete Element Method, Cellular Automata

1. Introduction

The impact damper is a type of vibration absorber that consists of a container attached to the primary vibrating structure. Additionally, it comprises a solid body constrained to move inside the container, where the damping effect can be obtained by collision and friction between the body and the container wall (Masri and Caughey 1966). The damper is usually used when an external damping treatment is substantially difficult, or when an extreme heat environment limits the use of viscous dampers. A particle damper is a type of an impact damper where the impact body is replaced by a granular assembly (Pannosian 1992). Establishing an effective numerical model is quite essential for the efficiency of the damper design for determining particle-related parameters, such as size, numbers, and material properties, which ultimately elicit the best damping performance.

The basic theoretical analyses deal with the particle bed as a single solid structure, which collides with the container wall plastically, whereby the dynamic response of the system is described by the governing equations of respective bodies (Friend and Kinra 2000; Papalou and Masri 1996). These approaches provide approximate predictions of the system behavior. However, the application is limited to simple systems, and the detailed information that may affect the system responses, such as the effect of particle size, or the friction between particles, cannot be fully modeled. Since the damper is intrinsically a nonlinear system, the continuum approximation approach could not be extended to the problems formulated at different scales.

On the other hand, the discrete element method (DEM) has been developed for modeling discontinuous materials, such as granular systems, in order to understand the microscopic behavior. In this case, the motion of each particle is numerically calculated by a set of motion equations considering the contact force between the elements. The early development of the model was introduced by Cundall and Struck in which the behavior of granular assemblies of discs and spheres was explained (Cundall and Strack 1979). Tsuji et al. extended Cundall's model to simulate the plug flow of spherical particles conveyed in a horizontal tube (Tsuji et al. 1992). They expressed the contact force between particles by using the Hertzian contact model. DEM has also been used to study the damping effect of the particle dampers. Saeki studied the relationship between the behavior of granules in the cavities, and the performance of a multi-unit particle damper using the Hertzian model in the DEM calculation (Saeki 2005). Other prior research studies refer to the modification of the contact model itself, or to the identification technique towards the precise estimation of the damping performance (Olson 2003; Wong et al. 2009; Malone and Xu 2008).

Since DEM employs governing equations on each grain, the behavior of individual particles and the gross motion of a granular system can be traced. However, the method requires a significant calculation time. This tremendously complex calculation is attributed to the setting of the simulation time step to a very small value in order for the impact calculation to be stable, and to particle-particle or particle-wall contact checks for all possible combinations. Reduction of the calculation time seems more significant than elaborating the

model-related parameters for the efficient damper design, especially in the case of predicting long-term, forced vibration responses. Mao et al. and Hu et al. introduced the link cell (LC) method, also known as the "box" algorithm, to reduce the number of contact checks (Mao et al. 2004; Hu et al. 2008). In the LC method, the space inside a container is divided into homogeneous cubic cells. By determining nonempty cells intersecting more than one particle, the contact detection was localized at the neighbors of the granules, which correspondingly reduced the frequency of contact checks. To further increase the contact detection efficiency, Fang et al. combined an improved LC method and an adaptively updated Verlet table that recorded all granular pairs whose distances were less than a predefined threshold value (Fang et al. 2007). Despite the improvement of computational efficiency, the procedure seems rather complex, and the management of the Verlet table might consume significant memory for an increasing number of particles.

Computer simulations using cellular automata (CA) may provide useful tools for understanding various types of phenomena in physical, social, and biological systems. CA models can produce complex patterns based on simple strategies describing behavior of elements, which are analogous to the appearance of complex systems (Chopard and Droz 1998; Ilachinski 2001). CA consist of finite-state variables arranged on uniformly segmented grids, each of which can vary within a finite set of values corresponding to the physical state of components in the system being analyzed. The time evolution of the system is updated synchronously according to the local interaction rule at every discrete time step. The state of a cell at a given time step only depends on its previous state and the state of nearby neighboring cells.

The CA modeling techniques provide advantages over the DEM approach in regard to computational efficiency and numerical stability, due to the local updating of variables, and the discrete treatment of time and space. CA has been used to model the particle behavior in granular flows (Prado and Olami 1992; Baxter and Behringer 1991; Sakaguchi et al. 1996). These studies have revealed that the CA model can describe any piece of physical properties, even with the use of simple rule definitions. However, few studies have qualitatively exploited the dynamic interactions between granular materials and a structure in CA models. This may have been due to the difficulty in relating discrete model parameters to the actual continuous physical quantities, such as the force, velocity, and others.

Towards an improved computational efficiency, we propose a new approach combining the DEM with the CA for modeling particles moving inside a granular damper container under the steady state forced excitation. We use the DEM to provide rigorous description of the physics related to the particle motion according to Newton's first law of motion, while the CA is introduced to reduce computational cost by limiting the contact checks of the local neighbors of each particle in cellular space. We also investigate the effect of simplification in the contact force model, which allows the unit time step of numerical integration to become relatively larger than the strict model, without causing numerical instability in the system calculation.

2. Measurement of the Damping Characteristics of a Granular Damper

We measured the damping characteristics of a granular damper experimentally in order to verify the numerical model using a fundamental DEM, as shown in the next section. A schematic of the experimental setup is shown in Fig. 1. An acrylic container is attached to the tip of two phosphor bronze plates, which constitute a base-excited, one degree-of-freedom (DOF) primary vibrating system constrained to move in the direction of gravity. The mass of the container is 88.6 g, and the natural frequency of the system is 6 Hz. The acrylic particles (6 mm in diameter, 0.2 g) are packed inside the container whose inner space dimensions are 96 mm in height, 60 mm in width, and 6 mm in thickness, in such a way that particles are restrained to move in two-dimensional space. The maximum number of particles that can be arranged in the vertical direction is 16, and 10 in the horizontal direction. The container is sinusoidally excited by an exciter at the clamped end of the leaf springs, with the constant base excitation amplitude of 2.0 mm. In this experiment, the damping performance was evaluated by measuring the absolute displacement of the primary system, where the number of particles varied from 0 to 60 at every 20 particles.

Fig. 2 shows the frequency responses of the primary system obtained by the experiment, where the particle damper incorporated a different number of particles. A root-mean-square (RMS) absolute displacement of the primary system is plotted against each excitation frequency. In the figure, the displacement is also expressed as the RMS transmissibility in non-dimensional form, where the absolute displacement is normalized by using the base excitation amplitude. It is shown that the damping effect increases in accordance to the particle number. The peak frequency shift towards the lower frequencies is mainly caused by the added mass effect of particles, which contributes to the decrease of the natural frequency.

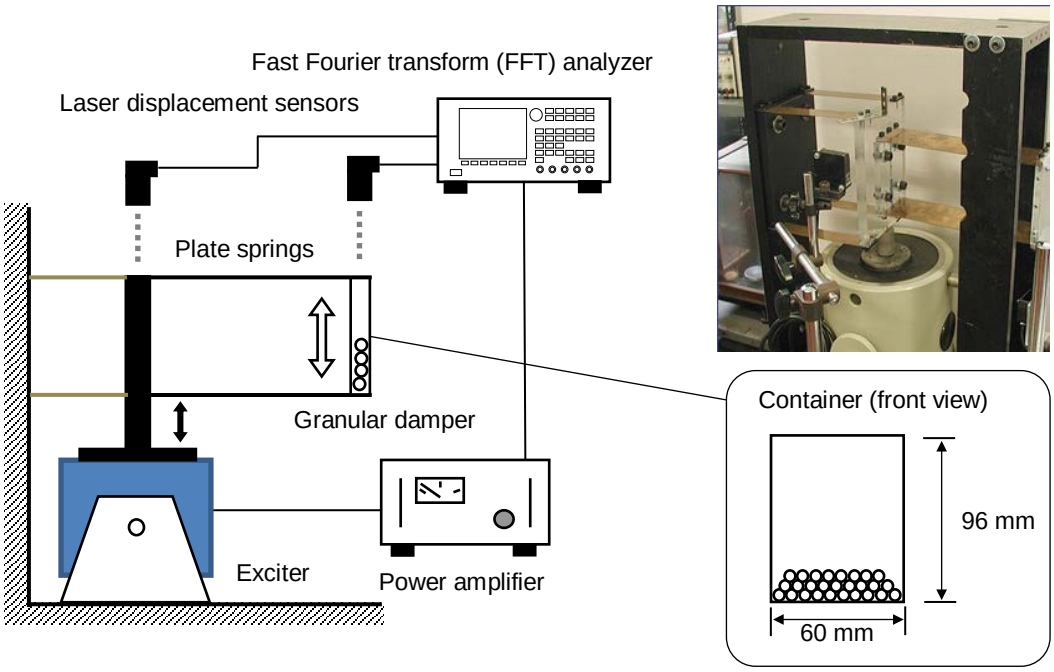

Fig. 1 Experimental setup of a vertically oriented granular damper

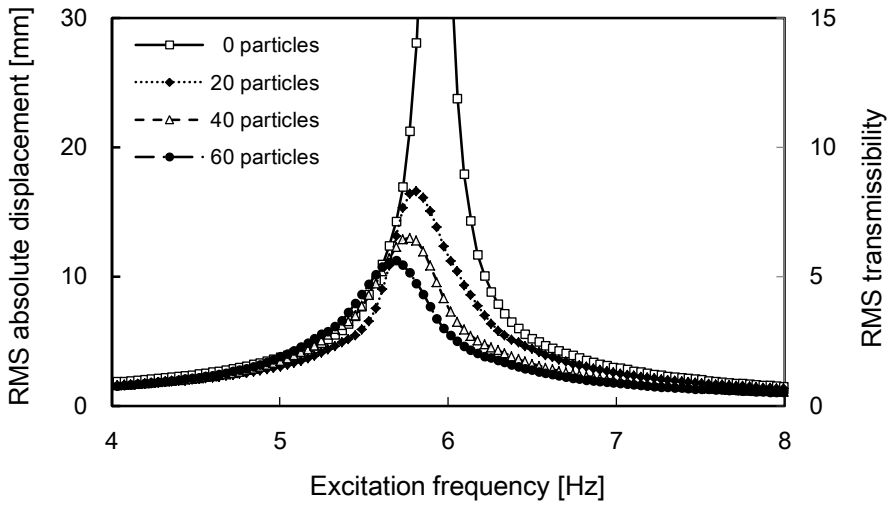

Fig. 2 Comparison of the damping effect as a function of the particle number (experimental results)

3. Modeling Particle Behavior Using a Strict Discrete Element Method

In this section, DEM is introduced to model the particle behavior inside the container when the system is excited harmonically. The DEM model consists of the governing equations defined for each particle considering the contact forces between the elements. The equations of motion for the particles and the primary system are described in this section.

3.1 A model of a primary system

If we consider x to be the displacement of the primary system in the vertical direction, the equation of motion for the primary system is written as follows:

$$M\ddot{x} + C\dot{x} + Kx = f_d + f_p \tag{1}$$

In Eq. (1), M, C, and K, represent the mass, damping coefficient, and spring constant of the primary system, respectively. Correspondingly, f_d denotes an external force acting on the primary mass, and f_p the total collision force brought in contact with particles. We investigated the harmonically-excited cases, where the force was defined as: $f_d\ (t) = F\sin 2\pi ft$. The force amplitude value F was 0.25 N, and the excitation frequency f was varied from 4 Hz to 8 Hz.

3.2 Equations for particle motion

When particles move within the two-dimensional space, three equations should be defined to describe their motion. Specifically, two translational equations for motion must be defined along the horizontal and vertical directions, and an equation for rotational motion with respect to the center of gravity. If particles are assumed to be spherical, and have uniform characteristics, the equations of motion for the i^{th} particle are represented by Eqs. (2) and (3).

$$m\ddot{\boldsymbol{p}}_i = \boldsymbol{F}_i - m\boldsymbol{g} \tag{2}$$

$$I\ddot{\varphi}_i = T_i \tag{3}$$

In Eqs. (2) and (3), m denotes the mass of the particle, I the moment of inertia, $\boldsymbol{p}_i$ the position vector, φ_i the angle of rotation, and $\boldsymbol{F}_i$ and T_i are the force and torque acting on a particle, respectively. In addition, $\boldsymbol{g}$ represents the acceleration of gravity. The contact force acting on a particle that is in contact with other particles, or with the container wall, can be decomposed into the normal and the tangential force components, f_n and f_t, respectively. These forces are explicitly expressed in conjunction with the normal and the tangential contact displacements, δ_n and δ_t, as follows (Tsuji et al. 1992):

$$f_n = k_p \delta_n^{\frac{3}{2}} + c_p \delta_n^{\frac{1}{4}} \dot{\delta}_n \tag{4}$$

$$f_t = \mu f_n \dot{\delta}_t / \left| \dot{\delta}_t \right| \tag{5}$$

In Eq. (4), c_p represents a damping coefficient, which is determined from the measured restitution coefficient, k_p is a spring constant derived using the Hertzian contact theory, and μ in Eq. (5) denotes the friction coefficient.

The spring constant k_p is defined in a different way, depending on whether a particle is in contact with another particle, or with a wall. If the particle is in contact with the wall, the spring constant k_{p1} is given as follows:

$$k_{p1} = \frac{4\sqrt{r}}{3} \frac{E \cdot E_0}{(1-\sigma^2)E_0 + (1-\sigma_0^2)E} \tag{6}$$

In the case of a collision between particles, the spring constant is defined by the following equation:

$$k_{p2} = \frac{\sqrt{2r}}{3} \cdot \frac{E}{(1-\sigma^2)} \tag{7}$$

In Eqs. (6) and (7), E and E_0 represent the Young's moduli, and σ and σ_0 the Poisson's ratios, of the particle and the wall, respectively, and r denotes the radius of the particle. The impact force f_p acting on the container wall is obtained by the summation of the x components of the normal and the tangential contact forces, f_n and f_t. In the same way, the x and y components of the force $\boldsymbol{F}_i$ that are exerted during the translational motions of the particle are calculated by the decomposition of f_n and f_t, and the synthesis of their components in the respective directions. The torque acting on a particle is also calculated by the radius r times the tangential force f_t.

In the fundamental DEM model, the contact between the particles is assessed for all the pairs irrespective of their separation distances. This process is thought to be a predominant cause of the computational load. The contact between the i^{th} and j^{th} particles is checked using their respective position vectors $\boldsymbol{p}_i$ and $\boldsymbol{p}_j$, and their radii r, as follows:

$$\left| \boldsymbol{p}_i - \boldsymbol{p}_j \right| < r \tag{8}$$

If Eq. (8) is satisfied for a given pair, the contact forces are then calculated using Eqs. (4) and (5).

3.3 Numerical prediction of the granular damper performance using a strict DEM model

In this subsection, the damping performance of the granular damper is evaluated numerically according to the strict DEM model described in the previous subsection. As shown in Fig. 3, the model of the damper consists of many particles packed inside a container. The container also works as a mass of the primary vibration system moving along the direction of gravity. Parameters used in the DEM analysis are shown in Table 1. To comply with experimental conditions, the inner dimension of the container was chosen to be 96 mm in height, 60 mm in width, and 6 mm in depth. The particle diameter was 6 mm, and hence, the particle motions inside the container were assumed to be two-dimensional. Material properties of an acrylic resin were considered for both the container and the particle. The forced response of the harmonically excited primary system was calculated, in which the number of particles varied from 0 to 60 at every 20 particles. In this case, the natural frequency of the primary system alone was approximately 6 Hz, and the time step for each calculation was dt = 2.0×10^{-5} s. The calculation step must be small enough in order to avoid numerical instability. The main cause of such instability is the collision between objects within a short time. Hence, the time step should be smaller than the contact duration T_c. In the present case, the time step dt was almost identical to $T_c/5$. Therefore, the total calculation time needed to obtain a response curve for a series of excitation frequencies becomes very large.

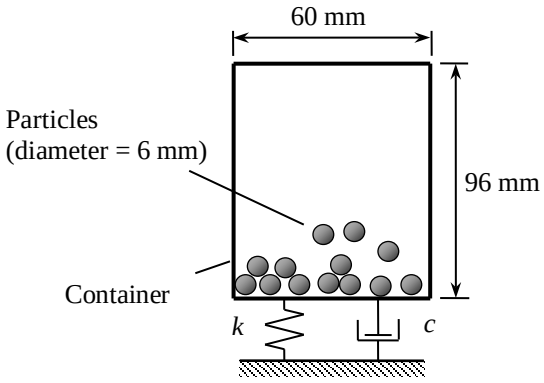

Fig. 3 Analytical model of the particle damper

Table 1 Parameters used in DEM calculation

Primary system	
Mass M	0.086 kg
Spring constant K	123.4 N/m
Damping coefficient C	0.08 Ns/m
Particle	
Mass m	0.2×10^{-3} kg
Radius r	3×10^{-3} m
Elastic constant E	0.4 GPa
Poisson's ratio σ	0.3
Friction coefficients μ_p, μ_w	0.2
Container	
Dimension	$0.096 \times 0.06 \times 0.006$ m^3
Elastic constant E_0	0.4 GPa

Poisson's Ratio σ_0	0.3

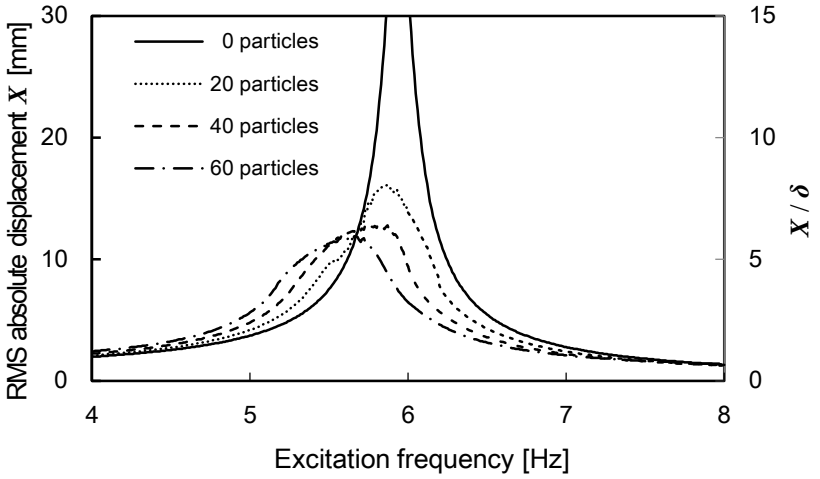

Fig. 4 Frequency response of the particle damper calculated by the DEM model

The numerical prediction result of the primary system response is shown in Fig. 4. The amplitude of the response curve is expressed by the RMS value where the time history of the absolute displacement at each excitation frequency is averaged over 40 periods. In the figure, the response is also expressed in non-dimensional form, where the RMS amplitude is normalized by using the static deflection value, $\delta = F / K$. In this case, the force amplitude F was 0.25 N, and the spring constant K of the primary system was 123.4 N/m. Hence the static deflection was calculated as δ = 2.0 mm. The results obtained are similar to the experimental observations, where the peak amplitude of the primary system is damped effectively as the number of particles increases. The peak frequency is also found to move towards a lower-frequency region depending on the number of particles.

4. Contact Detection Model using Cellular Automata

In the elementary DEM approach, an interparticle contact is usually checked for all combinations of particles, even if they are separated apart. Such a process seriously increases the total computational time for a large number of particles. In order to make the calculation more efficient, we investigate an approach combining the DEM with the CA for modeling particles moving inside a granular damper container. While we use DEM for modeling particle motions, which are governed by the physical law, CA is introduced for reducing computational cost by limiting the contact checks within the local neighboring region of each particle in cellular space. Specifically, particle displacements are treated as continuous values, and are numerically integrated in a rigorous manner using the Runge–Kutta method, obeying the equations of motion. At each moment, the calculated particle displacements along the x and y directions are further mapped onto the two-dimensional space. The indices used in the two directions correspond to discrete positions of particles in cellular space. We also investigate the effect of simplification in the contact force calculation, which allows the unit

time step of numerical integration to become relatively larger in comparison to the strict model, without destabilizing the system calculation.

4.1 Definition of discrete space for contact determination of particles

In this study, each compartment within a discrete space is called a cell. An example of the discrete space representation inside the container is shown in Fig. 5, in which the two-dimensional space is discretized into 32 rectangular cells vertically and 20 cells horizontally. Compared to the model shown in Fig. 1, the unit cell size corresponds to 3 mm. Thus, a particle having diameter of 6 mm occupies 2×2 cells. With reference to the origin (0, 0) assigned to a cell at the bottom left corner, the location of each cell is expressed by a combination of indices in both directions. Discrete representation of particle position along the two directions, i_x and i_y, is converted from the original real numbers x and y in accordance to,

$$\begin{cases} i_x = \max\{n \in Z \mid n < (N_x \times x / W + 0.5)\} \\ i_y = \max\{n \in Z \mid n < (N_y \times y / H + 0.5)\} \end{cases} \tag{9}$$

In Eq. (9), W and H denote the width and height of the container, N_x and N_y the indices of cells in horizontal and vertical directions, respectively. We assume that the particle center is located at a cell with the indices calculated a priori, although it does not always coincide with the true center due to the round-off errors in this conversion process. Herein, the size of a cell should be smaller than the radius of the particle in order to avoid overlapping of multiple particles at a single cell site. While the particle positions i_x and i_y are only used for the determination of inter-particle contact within the discrete space at each calculation step, the original position values x and y are consistently updated according to the DEM calculation. In the present investigation, three types of discrete cellular spaces are arranged, namely, 32×20, 64×40, and 128×80, and the effect of the spatial resolution on the calculation accuracy is evaluated.

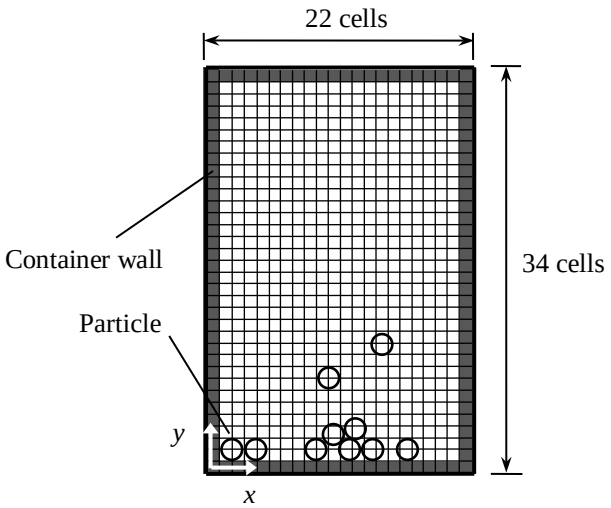

Fig. 5 Space discretization into cellular grids for the detection of contact between particles (example case of a 22×34 discretization)

4.2 Detection of contact between objects

Every particle center belongs to a particular cell center in space. In detecting the collisions between particles and other objects, the space is first searched sequentially for a cell having a particle center. If the cell is found, the surrounding neighboring area, whose thickness is as large as the diameter of the particle, is placed as shown in Fig. 6(a). The presence of other particles is subsequently scanned within the neighboring site in order to determine whether the interparticle collision will occur or not. Specifically, the four cells located near the central cell are excluded from the search since they cannot include a particle center. As shown in Fig. 6(b), a particle present within the region along the inner wall is considered to collide with the wall. Particle behavior is then updated by considering the collision force between the particle and the second object. The force is calculated according to the distance between the particle and the object.

Confinement of the contact search within the neighborhood of the particles reduces the computational time, especially for a large number of particles. Whereas the number of contact checks in one simulation cycle in an elementary DEM model is of the order of N^2 for N particles, in our model the contact number is of the order of $20 \times N$. The factor 20 corresponds to the number of neighbors that are scanned.

4.3 Modeling the collision force acting on particles

Since the particle collision is determined in the discretized cellular space, rigorous expression of the contact forces in Eqs. (4) and (5) may cause numerical instability under an approximate time-step setting. In addition, the precise expression, which requires a short time step, affects the total calculation time. Therefore, the impact dynamics are roughly approximated by the restitution coefficient instead of the expression of the sum of stiffness and damping forces. Friction between particles is further neglected for simplification. Thus, we only need to consider the momentum change in the normal direction, and the rotation of particles is not considered. These approximations allow the unit time step to become relatively large in comparison to the strict model, without causing numerical instability in the system calculation.

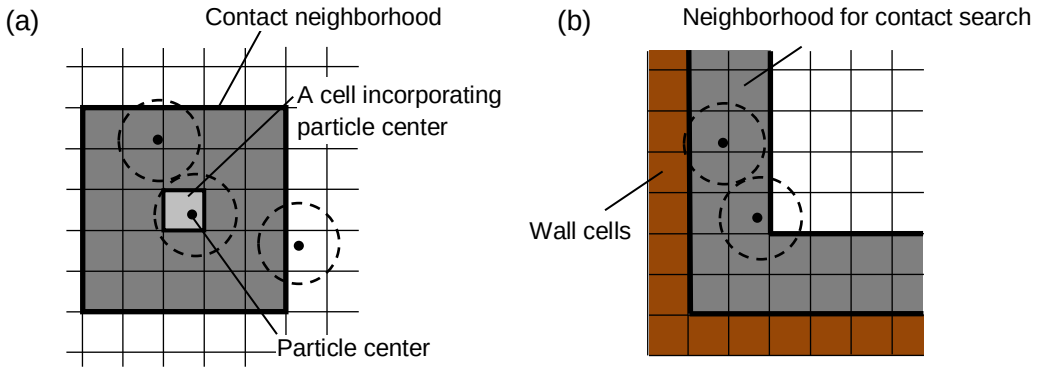

Fig. 6 Determination of collisions: (a) between particles, and (b) between particle and wall

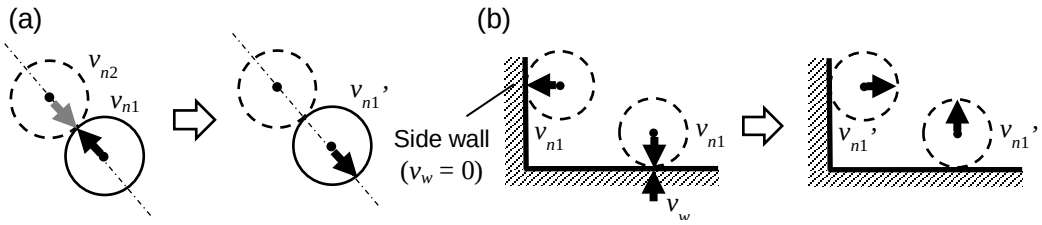

Fig. 7 Change of particle velocity upon collision: (a) against particle, and (b) against a wall

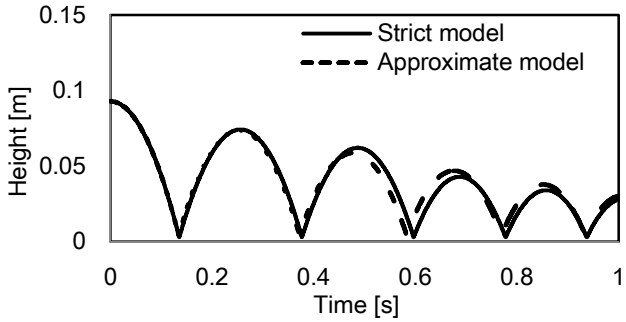

Fig. 8 The time history of a particle rebound against a flat plate is compared between two impact force representations. In the approximate model, the restitution coefficient e is taken to be equal to 0.75. The damping coefficient c_p in the strict DEM model is adjusted to fit the time trace of the approximate model

The particle velocity is first estimated according to the conservation of momentum before and after the collision. In the case of interparticle collision, as shown in Fig. 7(a), the particle velocity along the axis joining two particle centers is calculated by the following equation:

$$v'_{n1} = \frac{1}{2}\{(v_{n1} + v_{n2}) - e(v_{n1} - v_{n2})\} \tag{10}$$

In Eq. (10), v_{n1} and v'_{n1} respectively represent the particle velocities before and after the collision, v_{n2} the velocity of the other particle before the collision, and e the coefficient of restitution. In the case of the collision between a particle and a wall [Fig. 7(b)], the particle velocity is updated in accordance to

$$v'_{n1} = \frac{1}{m_p + m_w}\left\{(m_p - m_w e)v_{n1} + m_w(1+e)v_w\right\} \tag{11}$$

In Eq. (11), m_p and m_w, respectively represent the masses of the particle and the wall, v_{n1} corresponds to the velocity of the particle whose direction is normal to the wall, and v_w the velocity of the wall in the same direction. In addition, v_w is provided by numerically solving the equations of the primary system. Additionally, v_w always becomes zero at the side walls of the container, since head-on collisions between the particle and the side wall do not occur. The restitution coefficient that appeared in both Eqs. (10) and (11) is based on the rebound characteristic measurement for an acrylic particle against a flat acrylic plate.

In Fig. 8, the time history of a particle rebound motion against a flat surface is compared between the two impact force representations. In the approximate model, the restitution coefficient e is assumed to be equal to 0.75, whereas the damping coefficient c_p in the strict DEM model is adjusted to fit the time trace of the approximate model. Since the velocity update model described by Eqs. (10) and (11) only considers two-body collision, momentum exchange among many objects cannot be represented properly. Therefore, the impact force is further calculated from the momentum change towards the direction of collision for each combination of particles, in accordance to

$$f_{n1} = m_p \times (v'_{n1} - v_{n1}) / dt \tag{12}$$

In Eq. (12), dt represents the unit time step. The total force acting on a particle is calculated by adding every contribution of the impact force from the surrounding contacting particles. By further resolving the force vector into its x and y components in the global coordinate system, and substituting these into the force term in Eq. (2), the particle motion can be calculated. Similarly, the summation of the particle impact forces in contact with the container is also considered in the equation of the primary system [Eq. (1)].

5. Results and Discussion

5.1 Calculated response of the system using CA-based contact detection model

The primary system response of the granular damper is calculated using the CA-based contact detection model. The same condition as the strict DEM model is applied, but the contact force approximation model described in Section 4.3 is introduced. The two-dimensional space is divided into 32×20 cells, where the unit cell size corresponds to 3 mm. The calculation accuracy is investigated using two different time steps for the numerical integration, namely, dt = 2.0×10^{-5} s and 1.0×10^{-4} s. The calculated system responses whose values are presented in non-dimensional form are compared in Fig. 9. Despite the coarse setting of the unit time step in the latter case, little difference is found in these results for each particle number.

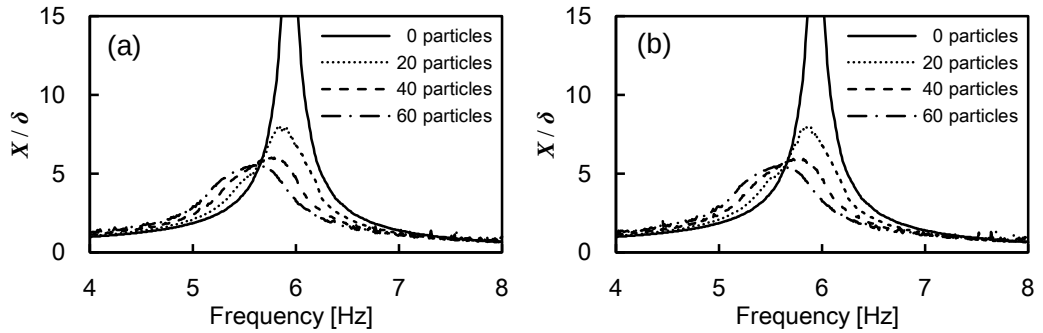

Fig. 9 Frequency responses of the particle damper calculated using the CA model. The two-dimensional space consists of 32×20 cells. The unit time step is set to: (a) $dt = 2.0\times10^{-5}$ s, and (b) $dt = 1.0\times10^{-4}$ s

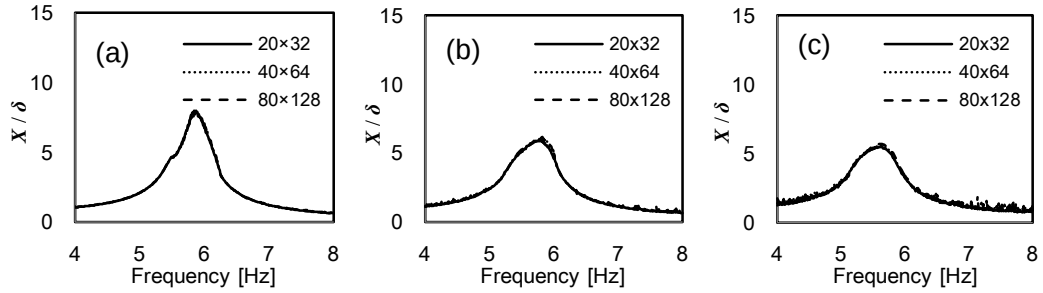

Fig. 10 Effects of the two-dimensional space grid division on the precision of the frequency response calculation. The number of particle is: (a) 20, (b) 40, and, (c) 60

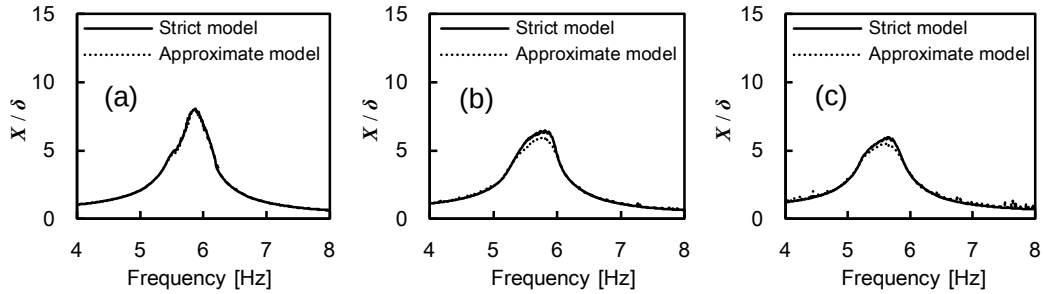

Fig. 11 Comparison of the calculation results between the strict DEM and approximate models. The time step is set to $dt = 2.0\times10^{-5}$ s in the strict model, and $dt = 1.0\times10^{-4}$ s in the approximate model. The number of particle is: (a) 20, (b) 40, and, (c) 60

The influence of the two-dimensional space division on the calculation accuracy is shown in Fig. 10, where three types of spatial resolutions are compared in regard to the response characteristics of the primary system incorporating respective particle numbers. The unit time step in these cases is set to $dt = 1.0\times10^{-4}$s. In every case, the response curves corresponded well to each other, regardless of the spatial resolution. The impact phenomenon ends instantaneously without causing numerical instability in the model, and the resolution of the spatial division rarely affects the determination of the interparticle contact as long as the time step is small enough compared to the minimum time needed for the particle to travel a unit

cell length.

As shown in Fig. 11, the responses of the primary system incorporating a different number of particles are further compared with the responses obtained by the strict DEM model. The discrete two-dimensional space is divided into 32×20 cells in the approximate model. Additionally, the time step used for the calculation is different in these models. Almost identical responses can be obtained using the approximate model. The slight difference in the response amplitude of the approximate model near the resonance is due to the overestimation of the contact forces. Discretizing the space at the higher resolution might not improve the accuracy under the coarse time step setting.

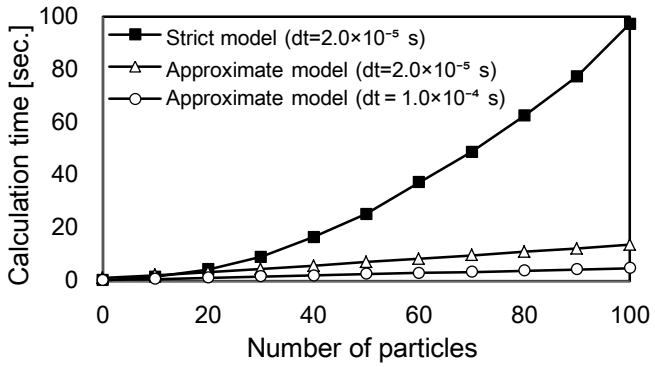

Fig. 12 Variation of calculation time against particle number

Table 2 Computing efficiency of the approximate model in comparison to the strict DEM model. The computing times were compared under the same time step condition: $dt = 2.0 \times 10^{-5}$

Number of particles	Computing time [s]		Efficiency ratio [%]
	Strict model	Approximate model	
20	4.4	3.3	134.0
40	16.6	5.7	288.8
60	37.3	8.4	445.6
80	62.5	11.0	568.8
100	97.2	13.7	710.5

5.2 Calculation time

The time required for system calculation in both the strict and the approximate models is compared in Fig. 12. The time step used for the numerical integration is equal to $dt = 2.0 \times 10^{-5}$ s, which is found to be the required marginal time step in order to obtain stable results for the strict model. In the approximate model, another time step, namely, $dt = 1.0 \times 10^{-4}$ s was considered. Increasing the particle numbers by 10, led to a measured increase in the actual time required for the computer to complete the five seconds of system response calculation. The tested hardware was equipped with a Core 2 Duo 3.0 GHz central processing unit (CPU), and a 2 GB main memory. A 32-bit Linux operating system was installed.

The calculation time required for strict DEM analysis becomes significantly large as the number of particles increases, while the time taken by the approximate model is much shorter. The difference becomes progressively large for an increasing number of particles. The

resultant calculation time in the strict model is quite dependent on the contact determination between objects, where the distance between every combination is calculated and examined within the two-dimensional space, even though some pairs are distant. On the other hand, since the contact search is only limited in the particle neighborhood sites in the approximate model, the time for computation is reduced significantly. The computing efficiency values of the approximate model are shown in percentage, in Table 2. The efficiency was defined as the ratio of the time required for the strict DEM model to the time for the approximate model, and the values were calculated for the time step condition: $dt = 2 \times 10^{-5}$ s. In terms of computational efficiency, the suggested approximation model is far more effective than the conventional DEM model, however, by an insignificant amount of degenerating calculation accuracy.

6. Conclusions

In the present study, we investigated a new approach combining the DEM with the CA for modeling the dynamic behavior of particles inside a vibrating damper container. While we used DEM to model the particle behavior using the equations of motion, the discrete cellular space was defined to limit the contact search within the local neighborhood of each particle. Additionally, a simplification was introduced on the representation of the contact force between the particles. It is shown that the computation becomes more efficient than the elementary DEM model, especially for a large number of particles, by introducing the particle contact scanning within a discrete cellular space. It is also shown that the suggested contact force approximation model allows a coarse setting of the unit time step, which contributes to the reduction of the computational time, and neither degenerates the calculation accuracy nor causes the numerical instability.

Acknowledgements

No funding or sponsorship was received for this study or publication of this article.

References

Baxter, G.W., Behringer, R.P.: Cellular automata models for the flow of granular materials. Physica D 51, 475–571 (1991)

Chopard, B., Droz, M.: Cellular Automata Modeling of Physical Systems. Cambridge University Press, Cambridge (1998)

Cundall, P.A., Strack, O.D.: A discrete numerical model for granular assemblies. Geotechnique 29, 47–65 (1979)

Fang, X., Tang, J., Luo, H.: Granular damping analysis using an improved discrete element approach. J. Sound Vib. 308, 112–131 (2007)

Friend, R.D., Kinra, V.K.: Particle impact damping. J. Sound Vib. 233(1), 93–118 (2000)

Hu, L., Huang, Q., Liu, Z.: A non-obstructive particle damping model of DEM. Int. J. Mech. Mater. Des. 4, 45–51 (2008)

Ilachinski A.: Cellular Automata: A Discrete Universe. World Scientific, Singapore (2001)

Malone, K.F., Xu, B.H.: Determination of contact parameters for discrete element method simulations of granular systems. Particulogy 6, 521–528 (2008)

Mao, K., Wang, M.Y., Xu, Z., Chen, T.: DEM simulation of particle damping. Powder Technol. 142, 154–165 (2004)

Masri, S., Caughey, T.: On the stability of the impact damper. J. Appl. Mech. 33(3), 586–592 (1966)

Olson, S.E.: An analytical particle damping model. J. Sound Vib. 26, 1155–1166 (2003)

Pannosian, H.V.: Structural damping enhancement via non-obstructive particle damping technique. J. Vib. Acoust. 114, 101–105 (1992)

Papalou, A., Masri, S. F.: Performance of particle dampers under random excitation. J. Vib. Acoust. 118, 614–621 (1996)

Prado C., Olami Z.: Inertia and break of self-organized criticality in sandpile cellular-automata models. Phys. Rev. A 45–2, 665–669 (1992)

Saeki, M.: Analytical study of multi-particle damping. J. Sound Vib. 281, 1133–1144 (2005)

Sakaguchi H., Murakami A., Hasegawa T., Shirai A.: Connected lattice cellular-automaton particles: A model for pattern formation in vibrating granular media. Soils Found. 36(1), 105–110 (1996)

Tsuji, Y., Tanaka, T., Ishida, T.: Lagrangian numerical simulation of plug flow of cohesionless particles in a horizontal pipe. Powder Technol. 71(3) 239–250 (1992)

Wong, C.X., Daniel, M.C., Rongong, J.A.: Energy dissipation prediction of particle dampers. J. Sound Vib. 319, 91–118 (2009)